Simulation of Semiconductor Processes and Devices 2016
Edited by E. Bär, J. Lorenz, and P. Pichler

Grain Boundary Resistance in Nanoscale Copper Interconnections

Daniel Valencia, Evan Wilson, Prasad Sarangapani, Gustavo A. Valencia-Zapata, Gerhard Klimeck, Michael Povolotskyi

Birck Nanotechnology Center
Purdue University
valencid@purdue.edu

Zhengping Jiang
Samsung Semiconductor Inc
San Jose, USA

***Abstract*— As logic devices continue to downscale, interconnections are reaching the nanoscale where quantum effects are important. In this work we introduce a semi-empirical method to describe the resistance of copper interconnections of the sizes predicted by ITRS roadmap. The resistance calculated by our method was benchmarked against DFT for single grain boundaries. We describe a computationally efficient method that matches DFT benchmarks within a few percent. The 1000x speed up compared to DFT allows us to describe grain boundaries with a 30 nm channel length that are too large to be simulated by ab-initio methods. The electrical resistance of these grain boundaries has a probability density distribution as a function of the grain rotation angles. This approach allows us to quantitatively obtain the most likely resistance for each configuration.**

Keywords—Copper interconnects, Extended Hückel method, coincident site lattice grain boundaries,

I. Introduction

As transistor sizes are scaled down, interconnect sizes must also be reduced. According to the ITRS roadmap, interconnects are expected to reach 10-20 nm in the next decade[1]. Earlier work by Fuchs and Mayadas[2], [3] has shown that surface and grain boundary (GB) scattering play a major role in the resistivity for structures of this size [4]. This study is based on a few empirical parameters but scaling factors limit their applications to simple orientations.

Recently first principles calculations have described the resistance of single grain boundaries based on a non-equilibrium Green function (DFT-NEGF) approach[5]. The results show a strong relationship between resistivity and the precise atomistic structure, which aligns both with experiments [6], [7] and previous theoretical work[8]. However, the studied structures are limited to single grain boundaries with less than two hundred atoms because of the computation cost of the DFT-NEGF calculation. To study larger grain boundaries, an accurate and efficient computational model is developed in this work.

II. Methodology

An atomistic, tight-binding method with a non-orthogonal basis based on the Extended Hückel (EH) tight-binding method[9] is used to describe copper interconnections. The EH parameters for copper were obtained from Cerdá and Soria [10] and benchmarked in two ways. First, the bulk band structure of copper obtained from the EH parametrization was compared to DFT as shown in Figure 1. The bulk band structure from DFT was calculated with the Atomistix ToolKit [11] for FCC copper with a lattice constant of 0.361 nm as reported experimentally[12]. All DFT calculations were performed with a generalized gradient approximation (GGA) and PBE functional with a k-sample generated by Monkhorst-Pack scheme of 10×10×10 and energy cutoff of 150 Ry.

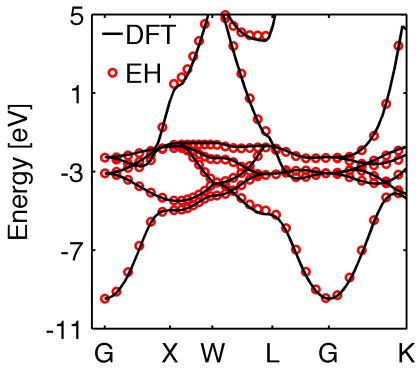

Figure 1: Band structure of bulk copper with DFT (lines) against EH (circles) making use of Cerda's parameters. The band diagrams show agreement between both models.

Secondly, single grain boundary systems were constructed and the transmission spectra and resistance of those grain boundaries were benchmarked against those calculated by DFT-NEGF. Single grain boundaries and in

particular coincident site lattice (CSL) grain boundaries were obtained by generating a superposition of two periodic lattices. One of the lattices was rotated with respect to the other, generating coincident points between the lattices for the specific rotation angle. This particular grain boundary is a special case of the general grain boundary. Still, it appears frequently in real interconnections because of the low interface energy[13]. High symmetry grain boundaries were constructed for structures smaller than two hundred atoms using the GBStudio package[14] (Figure 2 shows a Σ9 CSL grain boundary). The GBs were constructed from an FCC copper structure with a lattice constant equal to the value used for bulk calculations (0.361 nm). After generation, the CSL grain boundaries were structurally relaxed with DFT making use of the parameters as described above for the electronic calculations but with a k-sample of 4×4×1. The relaxation was carried out until all the atomic forces on each ion were less than 0.0001 eV nm^{-1}.

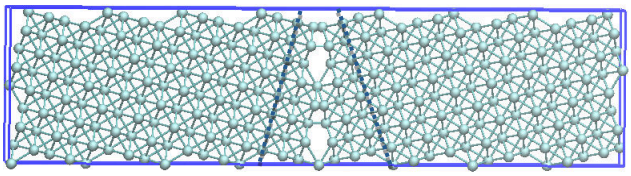

Figure 2: Representation of Coincident Site Lattice Σ9, the dashed lines indicate how the GB are created by a rotation of one of the lattices.

Subsequently, an electric potential of 2 meV was applied to the system and the ballistic resistance was obtained with Landauer's equation assuming a low bias condition:

$$\frac{1}{R} = \frac{e^2}{h} T(E_f) \qquad (1)$$

where e is the electron charge and T(E) is the transmission spectrum evaluated at the Fermi energy E_f. The transmission was calculated by the NEGF method for the non-orthogonal basis implemented in NEMO5[15] and benchmarked against the self-consistent NEGF+*ab-initio* in the Atomistix ToolKit. The Fermi level of the GB in the EH framework is calculated by integrating the density of states to find the total number of states as a function of energy. The states are then filled using a zero temperature approximation. For example, the density of states spectrum for a 1.6nm thick copper ultra-thin body with two periodic boundary conditions is shown in Figure 3(a). The total number of states as a function of energy Figure 3(b) is obtained by integration of the DOS spectrum.

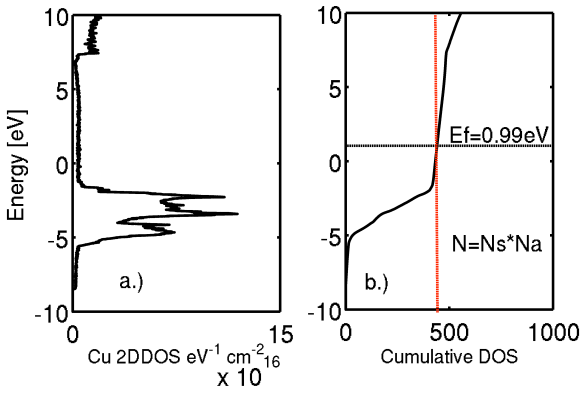

Figure 3 Extraction of the Fermi level from the DOS from a 1.6nm Cu ultra-thin body using the T= 0K approximation a.) DOS spectrum of the UTB b.) DOS is integrated up to the total number of states in the structure. In this case, 11 valence states per atom (N_s); 40 atoms (N_a) yields 440 states (N).

III. Result and Discussion

Making use of the NEGF method, the transmission spectra of several CSL grain boundaries were compared to those calculated in DFT for an energy range between -2 and 2 eV around the Fermi level. As shown in Figure 4, the transmission spectra for several CSL grain boundaries calculated by EH captures the main features of the DFT transmission spectra over a large energy window (not just near at E_F= 0eV).

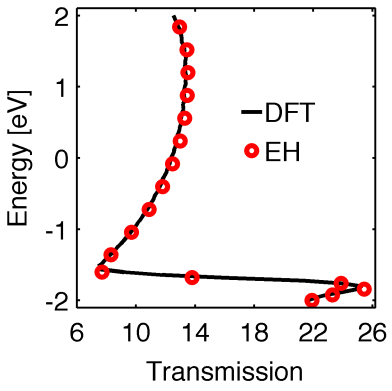

Figure 4: Transmission spectrum for Σ3 CSL computed using both DFT (lines) and EH (circles) methods.

Making use of equation (1), the resistances of several single grain boundaries were calculated as shown in Table 1. The results show that resistance calculated by EH method differs by less than 7% from the results obtained with DFT. This gives confidence that the method can be used for structures too large to simulate with DFT-NEGF. The time required to compute the transmission spectrum for both methods per CPU for a single energy and transverse wave vector is also tabulated in Table 2. The timing results show that EH offers a 10^3x speedup

compared to DFT+NEGF. These two tables show not only the accuracy of the EH's description of copper interconnects, but also that the EH approach allows for simulations of thousands of atoms to be completed in a reasonable time.

GB	Resistivity DFT(10^{-12} Ω cm^2)	Difference between EH and DFT (%)
Σ3	9.44	1.82
Σ5	10.41	3.98
Σ9	12.78	4.27
Σ11	9.60	0.38
Σ13	12.86	6.32

Table 1: Resistivities for different coincident lattices (Σ) calculated by EH and DFT differ by less than 7%

GB	Time DFT (s)	EH (s)
Σ3	19083.8	15.4
Σ5	26762.3	13.2
Σ9	27694.2	26.9
Σ11	511166.8	46.1

Table 2: Total time for different coincident lattices (Σ) calculated by EH and DFT

Large Grain Boundaries

After benchmarking our EH model against *ab-initio* calculations, large periodic grain boundaries were constructed as shown in Figure 5. The channel used for the GB was 30 nm long and had a 10nm x 1 unit cell cross-section as suggested in the ITRS roadmap[1]. The GB were grown in the [110] direction, which gives the highest conductance as previously reported in other studies[16].

Starting from a homogeneous [110] oriented structure, the multi-GB geometry was created according to the following steps: (1) generate scattered grain seeds; (2) create Voronoi cells using grain seeds; and (3) generate atoms inside grain boundaries. In this study, the GB channels were formed with three-grain boundaries that were rotated between 0 to 180 degrees as shown on figure5 b). After generation the GB channel was relaxed. Only non -*ab-initio* methods are available to relax structures of this size (more than 8 thousand atoms). Therefore a semi-classical EAM potential was applied[17] and benchmarked as well. However these results will be published soon.

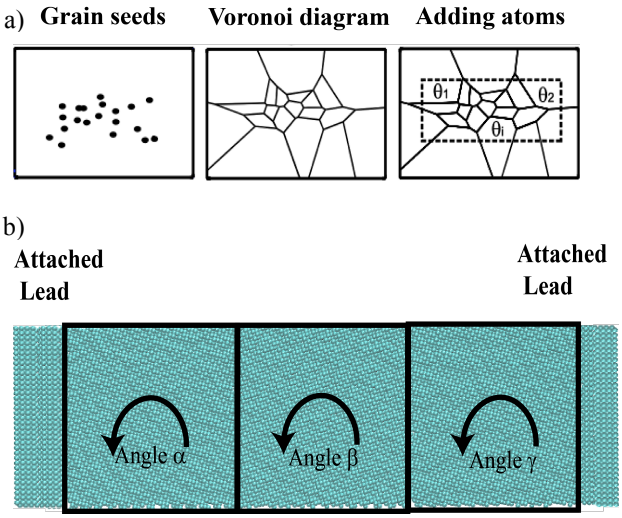

Figure 5 GB generation. (a) Generate random seed → Voronoi diagram → Divide original geometry into grains. (b) GB device with leads attached

Following the method outlined above, 600 GB structures were generated and their resistivities were calculated according to equation (1) for the EH method. The resistivity R was found to have a functional dependence on the rotation angles α,β,γ**.** Figure 6 shows the histogram overlaid with kernel density[18] curve for the resistivity R. The Shapiro-Wilk test showed the resistivity data does not follow a normal distribution with a 95% confidence[19].

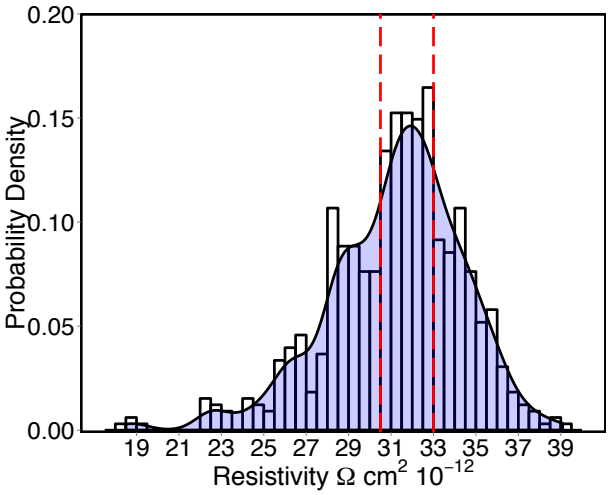

Figure 6. Multimodal distribution of resistivity. Values between 30.5 and 31 10^{-12} Ω cm^2 (indicated by red bars) have the highest probability.

As previously defined, the resistivity changes according to the variation of the three angles (α,β,γ). Figure 7 shows the resistivity distribution for different values of β. For instance, the boxplot presents the

resistance distribution as a function of β. The dependence on angle shows a mirror symmetry about 90^o. This result may be explained by the fact that the crystal symmetry of copper is not totally disrupted by the structural relaxation. Boxplot color was chosen in order to highlight the periodicity of the resistance with respect to the angle. It is important to mention that this symmetry pattern is the same for α and γ angles. Therefore, it is possible to identify the combination of angles that provide the highest resistance values. The maximum values of resistivity are most often in combinations of the following angles: $20^o, 60^o, 120^o$, and 160^o. In summary, the resistivity is to first order a periodic function of the grain boundary angles. To second order, particular arrangements of atoms can produce low-resistivity structures as show by the outliers in Figure 7.

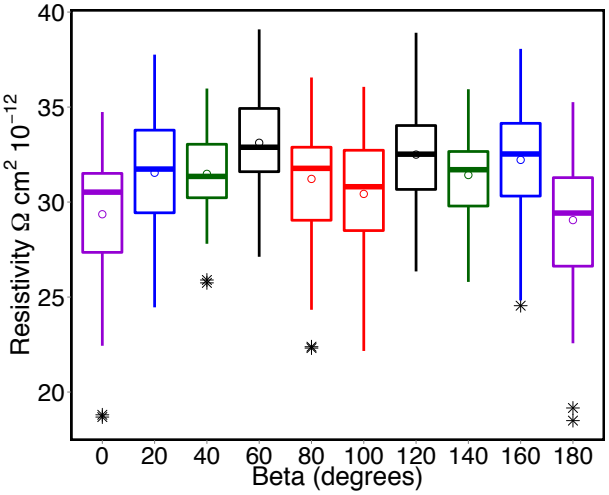

Figure 7. Resistivity distributions for angle β. The boxplots represent the resistance distribution, while those marked with a star represent outliers.

IV. Conclusions

In summary, a numerically effective method to calculate interconnect resistance was developed using a non-orthogonal tight binding technique. Subsequently, large grain boundaries were constructed and relaxed by EAM potential. The calculations for this approach are significantly faster and the results show agreement with *ab-initio* methods for CSL grain boundaries. In the case of large grain boundaries, the resistivity was found to have a functional dependence on the rotation angles α, β, γ that does not follow a normal distribution. Further studies will be performed to determine a relationship between the rotation of grain boundary and the resistivity using a statistical model that includes the quantitative effect of misalignment orientations and grain boundary size.

Acknowledgments

The authors acknowledge RCAC resources at Purdue University and Stampede machine at the Texas Advanced Computing Center under the project MCA08X012

References

[1] "International Roadmap for Semiconductors (ITRS)." 2014.

[2] K. Fuchs and N. F. Mott, "The conductivity of thin metallic films according to the electron theory of metals," *Math. Proc. Cambridge Philos. Soc.*, vol. 34, no. 01, p. 100, Jan. 1938.

[3] A. F. Mayadas, "Electrical Resisitivity model for polycrystalline films: The case of specular reflection at external surfaces," *Appl. Phys. Lett.*, vol. 14, no. 11, p. 345, Oct. 1969.

[4] R. L. Graham, G. B. Alers, T. Mountsier, N. Shamma, S. Dhuey, S. Cabrini, R. H. Geiss, D. T. Read, and S. Peddeti, "Resistivity dominated by surface scattering in sub-50 nm Cu wires," *Appl. Phys. Lett.*, vol. 96, no. 4, p. 042116, Jan. 2010.

[5] M. César, D. Liu, D. Gall, and H. Guo, "Calculated Resistances of Single Grain Boundaries in Copper," *Phys. Rev. Appl.*, vol. 2, no. 4, p. 044007, 2014.

[6] T.-H. Kim, X.-G. Zhang, D. M. Nicholson, B. M. Evans, N. S. Kulkarni, B. Radhakrishnan, E. A. Kenik, and A.-P. Li, "Large discrete resistance jump at grain boundary in copper nanowire.," *Nano Lett.*, vol. 10, no. 8, pp. 3096–100, Aug. 2010.

[7] L. Lu, Y. Shen, X. Chen, L. Qian, and K. Lu, "Ultrahigh strength and high electrical conductivity in copper.," *Science*, vol. 304, no. 5669, pp. 422–6, Apr. 2004.

[8] B. Zhou, Y. Xu, S. Wang, G. Zhou, and K. Xia, "An ab initio investigation on boundary resistance for metallic grains," *Solid State Commun.*, vol. 150, no. 29–30, pp. 1422–1424, Aug. 2010.

[9] R. Hoffmann, "An Extended Hückel Theory. I. Hydrocarbons," *J. Chem. Phys.*, vol. 39, no. 6, p. 1397, 1963.

[10] J. Cerdá and F. Soria, "Accurate and transferable extended Hückel-type tight-binding parameters," *Phys. Rev. B*, vol. 61, no. 12, pp. 7965–7971, Mar. 2000.

[11] M. Brandbyge, J.-L. Mozos, P. Ordejón, J. Taylor, and K. Stokbro, "Density-functional method for nonequilibrium electron transport," *Phys. Rev. B*, vol. 65, no. 16, p. 165401, Mar. 2002.

[12] M. E. Straumanis, L. S. Yu, and IUCr, "Lattice parameters, densities, expansion coefficients and perfection of structure of Cu and of Cu–In α phase," *Acta Crystallogr. Sect. A*, vol. 25, no. 6, pp. 676–682, Nov. 1969.

[13] Y. Kaneno and T. Takasugi, "Grain-boundary character distribution in recrystallized L12 ordered intermetallic alloys," *Metall. Mater. Trans. A*, vol. 34, no. 11, pp. 2429–2439, Nov. 2003.

[14] "GBStudio," *http://staff.aist.go.jp/h.ogawa/GBstudio/ (2003)*. .

[15] S. Steiger, M. Povolotskyi, H.-H. Park, T. Kubis, and G. Klimeck, "NEMO5: A Parallel Multiscale Nanoelectronics Modeling Tool," *Birck and NCN Publications*. 2011.

[16] G. Hegde, M. Povolotskyi, T. Kubis, T. Boykin, and G. Klimeck, "An environment-dependent semi-empirical tight binding model suitable for electron transport in bulk metals, metal alloys, metallic interfaces, and metallic nanostructures. I. Model and validation," *J. Appl. Phys.*, vol. 115, no. 12, p. 123703, Mar. 2014.

[17] Y. Mishin, M. J. Mehl, D. A. Papaconstantopoulos, A. F. Voter, and J. D. Kress, "Structural stability and lattice defects in copper: Ab initio , tight-binding, and embedded-atom calculations," *Phys. Rev. B*, vol. 63, no. 22, p. 224106, May 2001.

[18] Parzen Emanuel, "On Estimation of a Probability Density Function and Mode," *Ann. Math. Stat.*, vol. 33, no. 3, 1962.

[19] W. J. Conover, *Practical Nonparametric Statistics*, 3rd ed. 1999.